Hybrid Simulations of Multiple Islands in Magnetic Reconnection

Jianhua Cheng, Scott Parker, Yang Chen, Dmitri Uzdensky

University of Colorado-Boulder

Outline

- Model equations
- Second order semi-implicit method
- Multiple islands in large Δ' tearing mode
  - Secondary islands coalescence
  - Energy conversion
- Summary

Ion equations of motion and field equations

- Lorentz force ions

$$\frac{d\boldsymbol{v}_i}{dt} = \frac{q_i}{m_i}(\boldsymbol{E} + \boldsymbol{v}_i \times \boldsymbol{B})$$
$$\frac{d\boldsymbol{x}_i}{dt} = \boldsymbol{v}_i$$

- Ampere's equation

$$\bigtriangledown \times \boldsymbol{B} = \mu_0 \left(n_i q_i \boldsymbol{u}_i - n_e e \boldsymbol{u}_e\right)$$

- Faraday's law

$$\bigtriangledown \times \boldsymbol{E} = -\frac{\partial \boldsymbol{B}}{\partial t}$$

The generalized Ohm's law

- Starting from the electron momentum equation:

$$en_e(\boldsymbol{E} + \boldsymbol{u}_e \times \boldsymbol{B}) = en_e\eta\, \boldsymbol{j} - \bigtriangledown \cdot \mathbf{\Pi}_e - m_e\, \frac{\partial(n_e\boldsymbol{u}_e)}{\partial t}$$

where $\mathbf{\Pi}_e = \int f_e m_e \boldsymbol{v}\boldsymbol{v} d\boldsymbol{v}$.

- Substitute in Ampere's equation $\boldsymbol{j} = (n_i q_i \boldsymbol{u}_i - n_e e \boldsymbol{u}_e) = \frac{1}{\mu_0}\ \bigtriangledown \times \boldsymbol{B}$, the above equation could be rewritten as

$$en_e\boldsymbol{E} = -\boldsymbol{j}_i \times \boldsymbol{B} + \frac{1}{\mu_0}\,(\bigtriangledown \times \boldsymbol{B}) \times \boldsymbol{B} + \frac{en_e}{\mu_0}\,\eta\,(\bigtriangledown \times \boldsymbol{B}) - \bigtriangledown \cdot \mathbf{\Pi}_e - m_e\,\frac{\partial(n_e\boldsymbol{u}_e)}{\partial t}$$

where $\boldsymbol{j}_i = n_i q_i \boldsymbol{u}_i$.

Electron inertia

- Taking the time derivative of Ampere's equation

$$\mu_0 \left(q_i \frac{\partial n_i \boldsymbol{u}_i}{\partial t} - e \frac{\partial n_e \boldsymbol{u}_e}{\partial t} \right) = \nabla \times \frac{\partial \boldsymbol{B}}{\partial t} = - \nabla \times \nabla \times \boldsymbol{E}$$

- The first term on the left hand side is obtained from the ion momentum equation, thus the electron inertial term can be written as

$$m_e \frac{\partial (n_e \boldsymbol{u}_e)}{\partial t} = \frac{m_e}{m_i} \frac{q_i}{e} \left(q_i n_i (\boldsymbol{E} + \boldsymbol{u}_i \times \boldsymbol{B}) - \nabla \cdot \boldsymbol{\Pi}_i - q_i n_i \frac{\eta}{\mu_0} \nabla \times \boldsymbol{B} \right) + \frac{m_e}{\mu_0 e} \nabla \times \nabla \times \boldsymbol{E}.$$

Generalized Ohm's law

- Using quasi-neutrality $n_i = n_e$, the electron density and flow can be calculated directly from particle ions

$$
\begin{aligned}
& en_i(1+\frac{m_e}{m_i}\frac{q_i^2}{e^2})\boldsymbol{E}+\frac{m_e}{\mu_0 e}\bigtriangledown\times(\bigtriangledown\times\boldsymbol{E}) \\
= & -(1+\frac{m_e}{m_i}\frac{q_i}{e})\,\boldsymbol{j}_i\times\boldsymbol{B}+\frac{1}{\mu_0}(\bigtriangledown\times\boldsymbol{B})\times\boldsymbol{B} \\
& +\eta\frac{en_i}{\mu_0}(1+\frac{m_e}{m_i}\frac{q_i^2}{e^2})\bigtriangledown\times\boldsymbol{B}-\nabla\cdot\boldsymbol{\Pi}_e+\frac{m_e}{m_i}\frac{q_i}{e}\,\nabla\cdot\boldsymbol{\Pi}_i,
\end{aligned}
$$

- In general, we need an electron model to calculate Π_e. Here we assume the electrons are isothermal and Π_e reduces to

$$P_e = n_e T_e = n_i T_e$$

Future plans include drift-kinetic and gyro-kinetic electron models.

The second-order semi-implicit δf algorithm

- In order to eliminate the fast compressional wave, we have implemented a second-order accurate semi-implicit method.

- For particle ions, the usual δf method is employed. Given a distribution function $f = f_0 + \delta f$, if a weight of $w_j = \frac{\delta f}{f}|_{x=x_j,v=v_j}$ is assigned to each particle, we could then calculate the field quantities by weight δf to the grids. According to Vlasov equation, the particle weight evolves as

$$\frac{d}{dt}w_j = -\frac{d\ln f_0}{dt}|_{x=x_j,v=v_j}$$

Yang Chen, Scott E. Parker, Phys. Plasmas **16**, 052305 (2009)

Second order semi-implicit scheme

- The velocity, length and time are normalized to $c_s^2 = T_e/m_i$, $\rho_s = m_i c_s/eB_0$ and $\Omega_{ci}^{-1} = m_i/eB_0$. $\beta_e = \mu_0 n_0 T_e/B_0^2$ is defined upon the uniform background plasma.
- The equations of motion are

$$\frac{\boldsymbol{x}^{n+1} - \boldsymbol{x}^n}{\Delta t} = (1-\theta)\ \boldsymbol{v}^n + \theta\ \boldsymbol{v}^{n+1},$$
$$\frac{\boldsymbol{v}^{n+1} - \boldsymbol{v}^n}{\Delta t} = (1-\theta)\ \boldsymbol{a}^n + \theta\ \boldsymbol{a}^{n+1},$$
$$\frac{w^{n+1} - w^n}{\Delta t} = -(1-\theta)\ (\boldsymbol{v}^n \cdot \bigtriangledown + \boldsymbol{a}^n \cdot \partial_{\boldsymbol{v}}) \ln f_0(\boldsymbol{x}^n, \boldsymbol{v}^n)$$
$$-\theta\ (\boldsymbol{v}^{n+1} \cdot \bigtriangledown + \boldsymbol{a}^{n+1} \cdot \partial_{\boldsymbol{v}}) \ln f_0(\boldsymbol{x}^{n+1}, \boldsymbol{v}^{n+1}),$$

  where $\boldsymbol{a} = \frac{q_i}{m_i}(\boldsymbol{E} + \boldsymbol{v} \times \boldsymbol{B})$.
- Generalized Ohm's law:

$$(n_{i0} + \delta n_i^{n+1})(1 + \frac{m_e}{m_i} q_i^2)\boldsymbol{E}^{n+1} + \frac{m_e}{m_i}\frac{1}{\beta_e} \bigtriangledown \times(\bigtriangledown \times \boldsymbol{E}^{n+1})$$
$$= -(1 + \frac{m_e}{m_i} q_i)\delta \boldsymbol{j}_i^{n+1} \times (\boldsymbol{B}_0 + \delta \boldsymbol{B}^{n+1}) + \frac{1}{\beta_e}(\bigtriangledown \times \delta \boldsymbol{B}^{n+1}) \times \boldsymbol{B}_0$$
$$+\frac{1}{\beta_e}(\bigtriangledown \times (\boldsymbol{B}_0 + \delta \boldsymbol{B}^{n+1})) \times \delta \boldsymbol{B}^{n+1} + \frac{\eta}{\beta_e}(1 + \frac{m_e}{m_i} q_i^2)(n_{i0} + \delta n_i^{n+1}) \bigtriangledown \times \delta \boldsymbol{B}^{n+1}$$
$$-\nabla \delta n_i^{n+1} + \frac{m_e}{m_i} q_i\ \bigtriangledown \cdot P_i^{n+1},$$

Ion current and nonlinear terms

- The first term on the right hand side of the generalized Ohm's law involves the future ion current density

$$e n_i (1 + \frac{m_e}{m_i}\frac{q_i^2}{e^2}) \boldsymbol{E}^{n+1} + \cdots = -(1 + \frac{m_e}{m_i}\frac{q_i}{e})\ \delta \boldsymbol{j}_i^{n+1} \times \boldsymbol{B}^{n+1} + \cdots$$

  we approximate $\delta \boldsymbol{j}_i^{n+1}$ as follows

$$\begin{aligned}
\delta \boldsymbol{j}_i^{n+1} &= q_i \sum_j w_j^{n+1} \boldsymbol{v}_j^{n+1} \\
&= \delta \boldsymbol{j}_i^{\star} + q_i\ \theta\ \Delta t \sum_j \frac{q_i}{T_i} \boldsymbol{E}^{n+1}(\boldsymbol{x}_j^{n+1}) \cdot \boldsymbol{v}_j^{n+1} \boldsymbol{v}_j^{n+1} \\
&\simeq \delta \boldsymbol{j}_i^{\star} + \theta\ \Delta t\ \frac{q_i^2}{m_i}\ \boldsymbol{E}^{n+1} \equiv \boldsymbol{J}_i'.
\end{aligned}$$

- For accuracy issues, we iterate on the differences between $\delta \boldsymbol{j}_i^{n+1}$ and $\boldsymbol{J}_i'$.
- For every k_y and k_z mode, the generalized Ohm's law is solved in x direction using finite difference. The equilibrium part is solved by direct matrix inversion. And the nonlinear terms are treated iteratively.

Benchmarks

- We have carefully benchmarked the code with the Alfven waves, whistler waves and ion acoustic waves with linear Landau damping. We have also investigated the small Δ' tearing mode and the simulation is consistent with the MHD studies. The results are summarised in the paper submitted to JCP.

Equilibrium and Boundary conditions

- Zero-order magnetic field $\boldsymbol{B}_0(\boldsymbol{x}) = B_{y0} \tanh(\frac{x}{a})\ \hat{\boldsymbol{y}} + B_G\ \hat{\boldsymbol{z}}$

- Perfect conducting wall boundary condition is employed in x while periodic boundary conditions in y and z direction.

$$\boldsymbol{E}_{y,z}|_{x=\pm l_x/2} = 0$$
$$\delta \boldsymbol{B}_x|_{x=\pm l_x/2} = 0$$

- Particles are reflected at $x = \pm l_x/2$.

Island evolution I

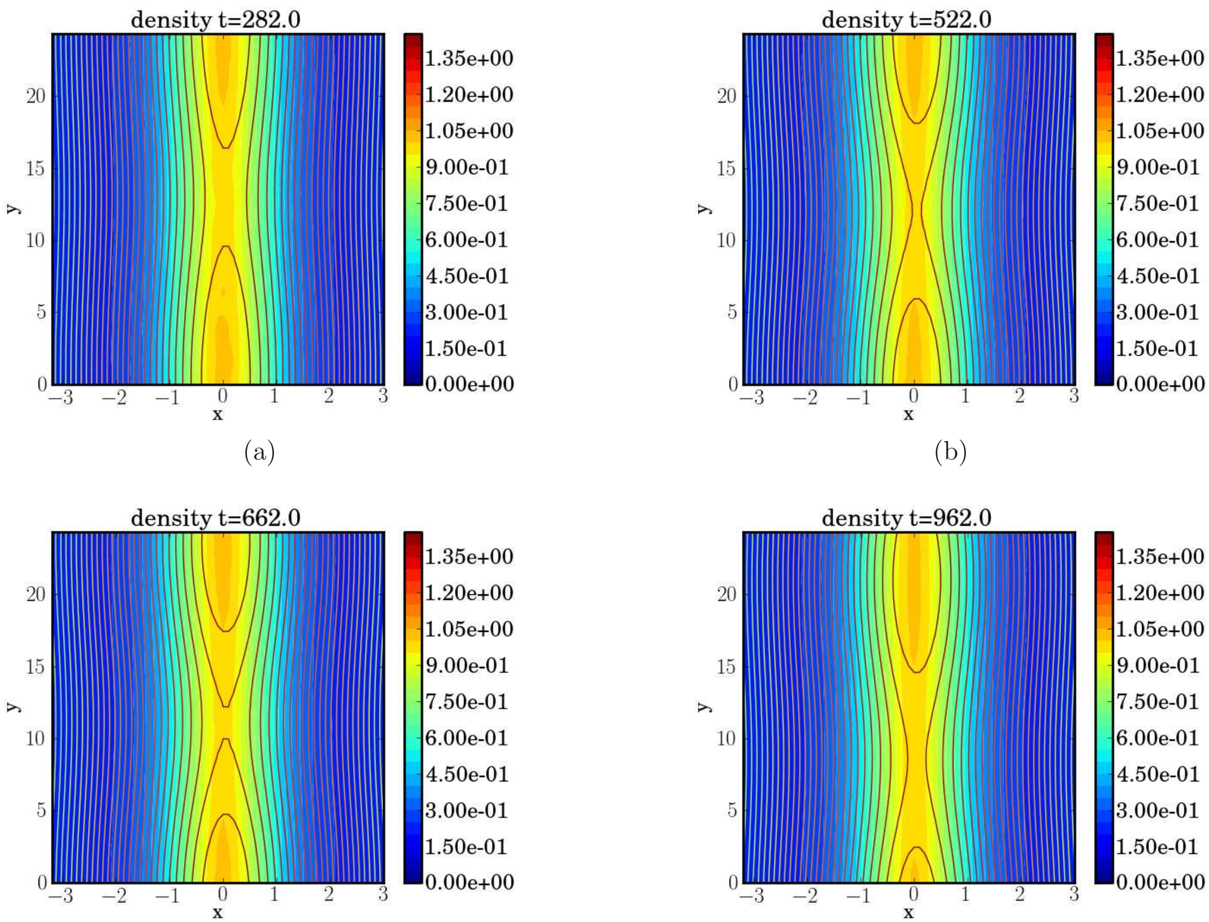

(a) (b)

(c) (d)

$128 \times 64 \times 16$ grids, 1048576 particles. $\frac{a}{\rho_i} = 1.0, \beta_e = \frac{\mu_0 n_0 T_e}{B_0^2} = 0.5$,
$\eta \frac{e n_0}{B_0} = 15 \times 10^{-4}$, $\frac{\boldsymbol{B}_G}{B_0} = 0$, $\frac{T_i}{T_e} = 1$, $\frac{l_x}{\rho_i} = 12.8$, $\frac{l_y}{\rho_i} = 25.12$

Island evolution II

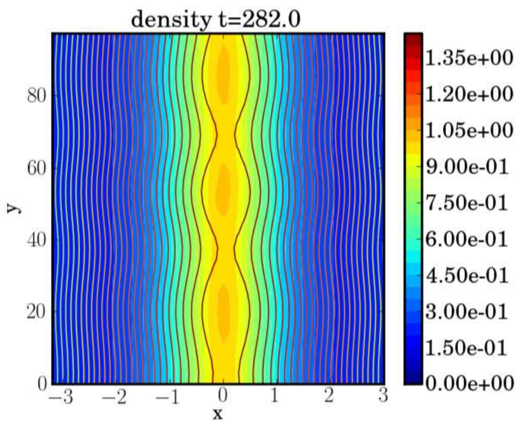

(a)

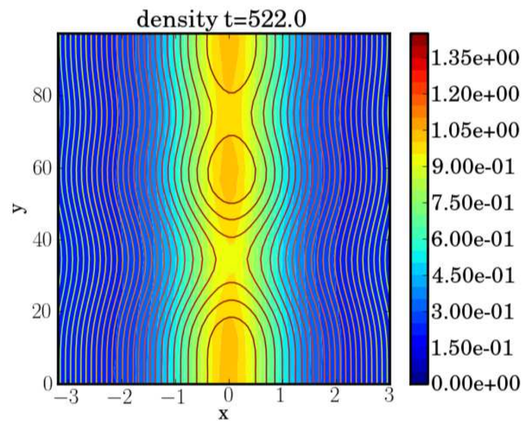

(b)

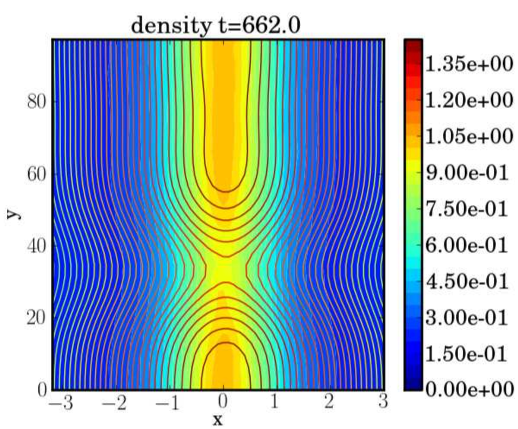

(c)

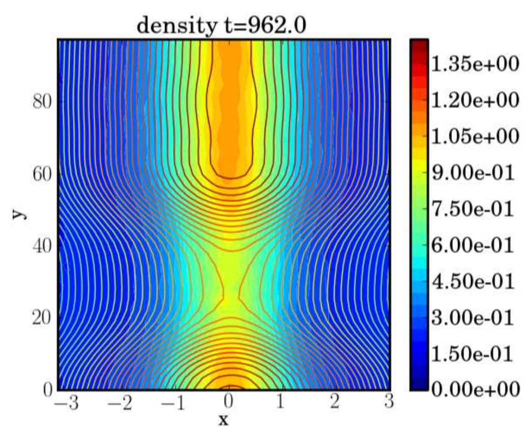

(d)

$128 \times 64 \times 16$ grids, 1048576 particles. $\frac{a}{\rho_i} = 1.0, \beta_e = \frac{\mu_0 n_0 T_e}{B_0^2} = 0.5,$
$\eta \frac{e n_0}{B_0} = 15 \times 10^{-4}, \frac{\boldsymbol{B}_G}{B_0} = 0, \frac{T_i}{T_e} = 1, \frac{l_x}{\rho_i} = 12.8, \frac{l_y}{\rho_i} = 100.48$

Island width with different aspect ratio

- Island growth with various aspect ratio.

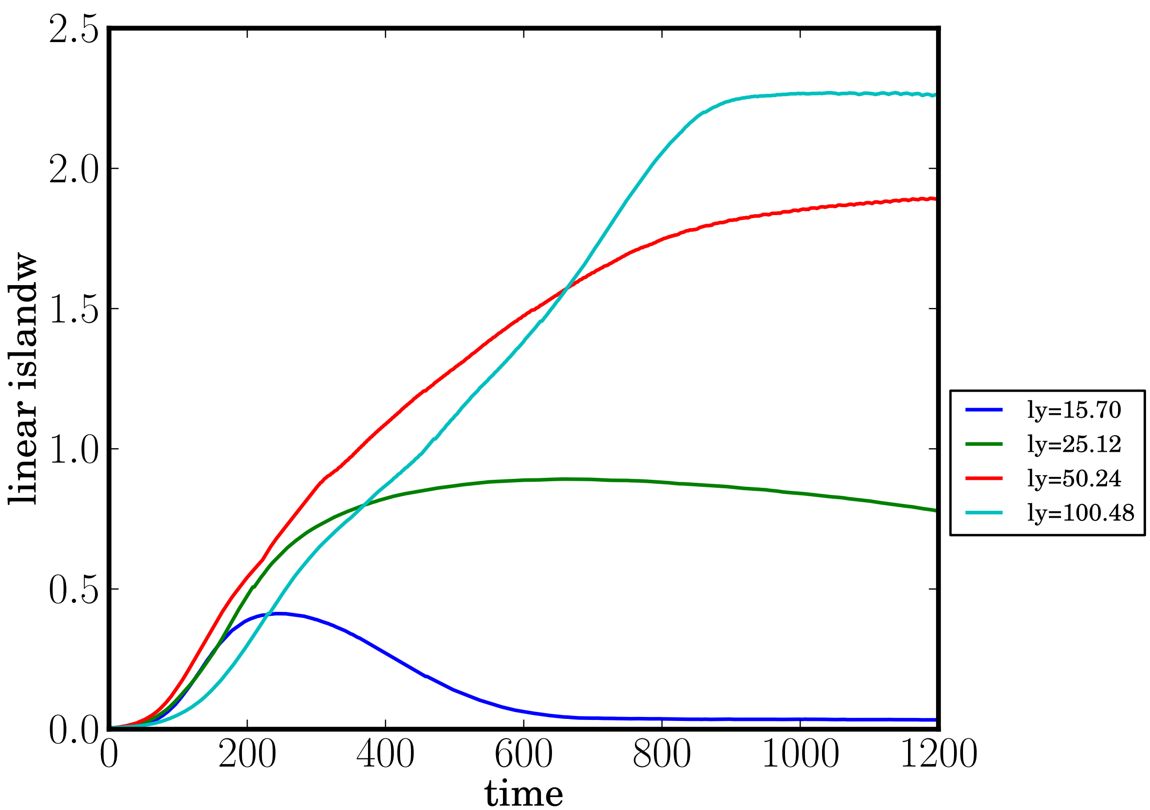

$128 \times 64 \times 16$ grids, 1048576 particles. $\frac{a}{\rho_i} = 1.0, \beta_e = \frac{\mu_0 n_0 T_e}{B_0^2} = 0.5, \frac{\boldsymbol{B}_G}{B_0} = 0, \frac{T_i}{T_e} = 1, \frac{l_x}{\rho_i} = 12.8$

Energy conservation

- Take the second moment of the Vlasov equation, we have

$$\frac{\partial}{\partial t}(KE) = \int \boldsymbol{E} \cdot \boldsymbol{j}_i \, d^3\boldsymbol{x}.$$

- With the generalized Ohm's law, the rhs is rewritten as

$$\begin{aligned}\int \boldsymbol{E} \cdot \boldsymbol{j}_i \, d^3\boldsymbol{x} = & -\frac{1}{2\mu_0}\frac{\partial}{\partial t}\int \boldsymbol{B}^2 \, d^3\boldsymbol{x} - \int \frac{1}{\boldsymbol{B}^2}\left[(\frac{1}{\mu_0}\nabla \times \boldsymbol{B} - \boldsymbol{j}_i) \cdot \boldsymbol{B}\right] \boldsymbol{B} \cdot \boldsymbol{E} \, d^3\boldsymbol{x} \\ & -\int \frac{\eta e n_0}{\mu_0}\frac{1}{\boldsymbol{B}^2}\nabla \times \boldsymbol{B} \times \boldsymbol{B} \cdot \boldsymbol{E} \, d^3\boldsymbol{x} + \int \frac{1}{\boldsymbol{B}^2}\nabla \cdot \boldsymbol{\Pi}_e \times \boldsymbol{B} \cdot \boldsymbol{E} \, d^3\boldsymbol{x} \\ & + m_e \int \frac{1}{\boldsymbol{B}^2}\frac{\partial n_e \boldsymbol{u}_e}{\partial t} \times \boldsymbol{B} \cdot \boldsymbol{E} \, d^3\boldsymbol{x},\end{aligned}$$

Magnetic energy and Ion kinetic energy

- The kinetic energy and magnetic energy change in the simulation

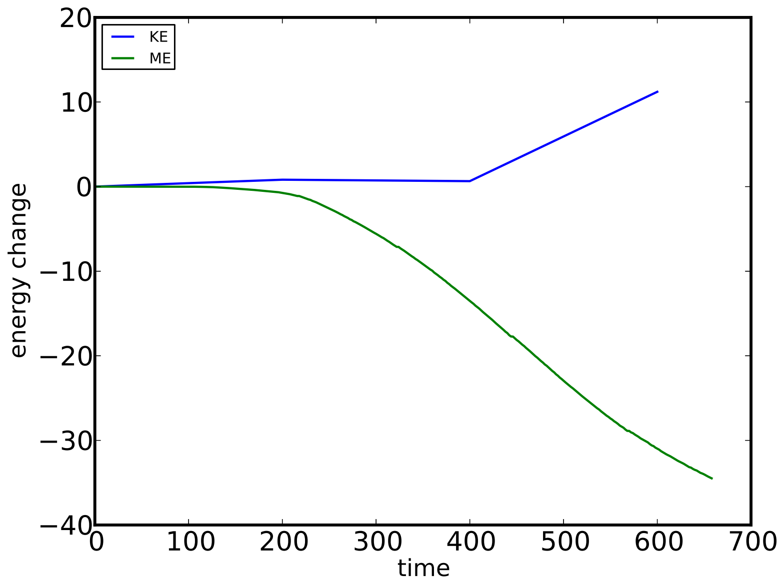

(a)

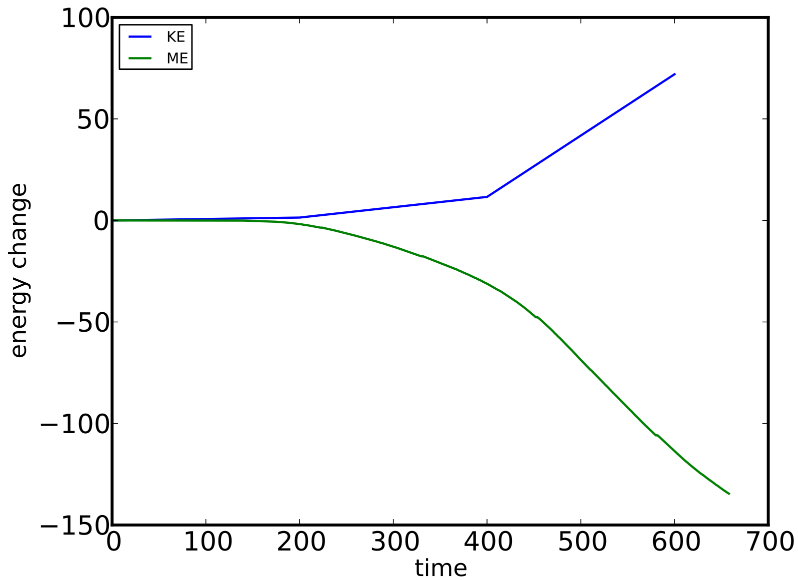

(b)

(a) $\frac{l_y}{\rho_i} = 50.24$. (b) $\frac{l_y}{\rho_i} = 100.48$

$128 \times 64 \times 16$ grids, 1048576 particles. $\frac{a}{\rho_i} = 1.0, \beta_e = \frac{\mu_0 n_0 T_e}{B_0^2} = 0.5$,

$\eta \frac{e n_0}{B_0} = 15 \times 10^{-4}, \frac{\boldsymbol{B}_G}{B_0} = 0, \frac{T_i}{T_e} = 1, \frac{l_x}{\rho_i} = 12.8$

Ion heating in the island region

- The distribution function clearly shows that ions are heated.

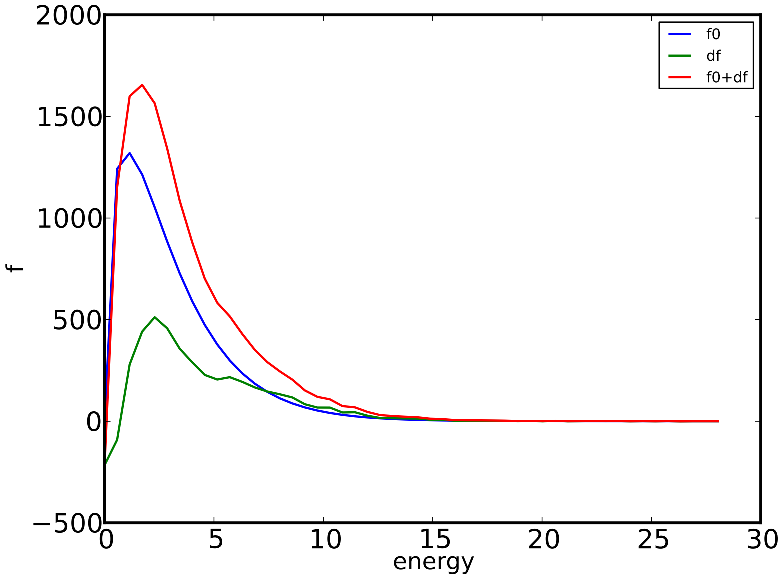

(a)

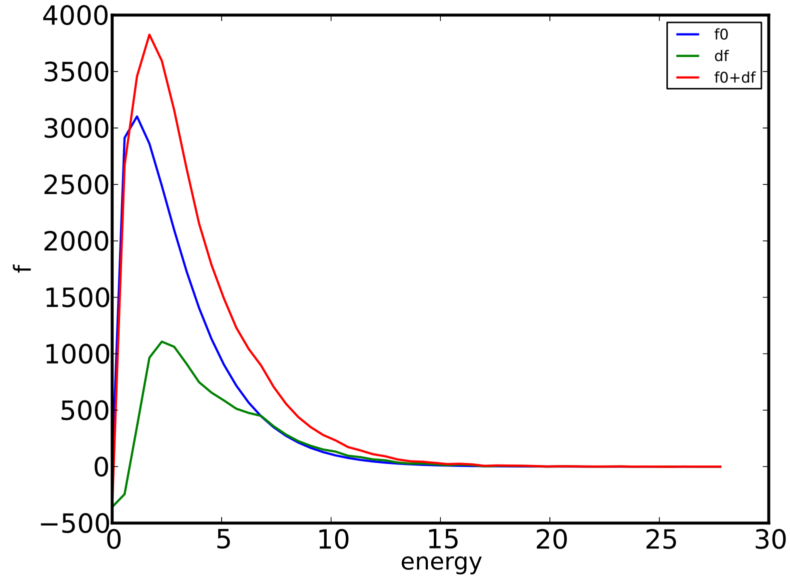

(b)

(a) $t = 400\Omega_i^-1$ (b) $t = 600\Omega_i^-1$

$128 \times 64 \times 16$ grids, 1048576 particles.

$\frac{a}{\rho_i} = 1.0, \beta_e = \frac{\mu_0 n_0 T_e}{B_0^2} = 0.5, \frac{\boldsymbol{B}_G}{B_0} = 0, \frac{T_i}{T_e} = 1, \frac{l_x}{\rho_i} = 12.8, \eta = 0.0015, \frac{l_y}{\rho_i} = 100.48$

Average kinetic energy of ions in the island region

- Looking into the island region, the average kinetic energy of ions increases about 13%.

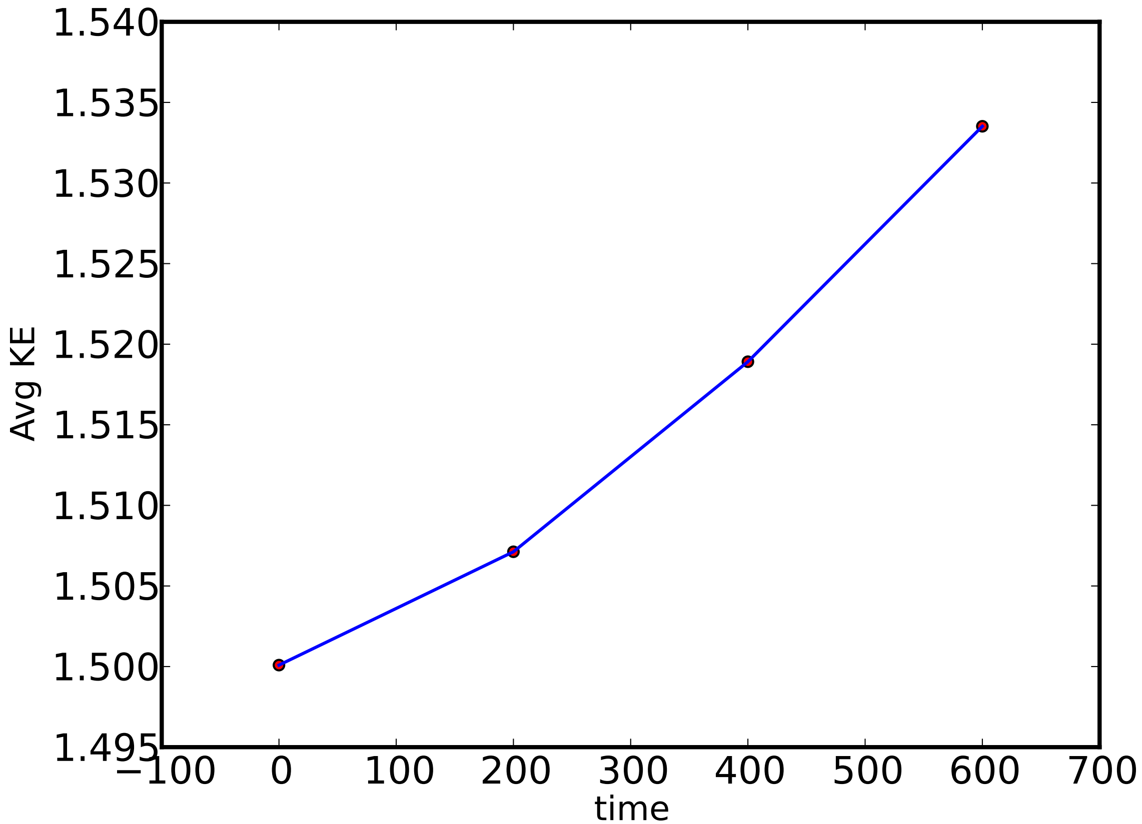

$128 \times 64 \times 16$ grids, 1048576 particles.

$\frac{a}{\rho_i} = 1.0, \beta_e = \frac{\mu_0 n_0 T_e}{B_0^2} = 0.5, \frac{\boldsymbol{B}_G}{B_0} = 0, \frac{T_i}{T_e} = 1, \frac{l_x}{\rho_i} = 12.8, \eta = 0.0015, \frac{l_y}{\rho_i} = 100.48$

Summary

1. We have implemented a second-order accurate implicit algorithm with Lorentz force ions and isothermal fluid electrons which is
   - Quasi-neutral and fully electromagnetic.
   - Suitable for MHD scale plasmas.

2. Secondary islands in the strong tearing mode.
   - For large Δ' tearing mode, we have observed multiple islands forming and coalescence.
   - Using particle ion diagnostics, we have shown that ions are heated in the island region and compared with the magnetic energy change.

3. Future work
   - Further detailed diagnostics about the energy conversion in the process.
   - Use tracer particles to study the particle behaviors (e. g. dissipation) around the X and O points of the islands.